AIAA JOURNAL
Vol. 31, No. 12, December 1993

Diverging Boundary Layers with Zero Streamwise Pressure Gradient and No Wall Curvature

Wayne R. Pauley*
Pennsylvania State University, University Park, Pennsylvania 16802
John K. Eaton†
Stanford University, Stanford, California 94305
and
Andrew D. Cutler‡
George Washington University JIAFS/NASA Langley Research Center, Hampton, Virginia 23665

The effects of spanwise divergence ($\partial W/\partial z$) on the boundary layer forming between a pair of embedded streamwise vortices with the common flow between them directed toward the wall was studied. Measurements indicate that divergence controls the rate of development of the boundary layer and that large divergence significantly retards boundary-layer growth and enhances skin friction in agreement with previous studies. Even with divergence, however, the local similarity relationships for two-dimensional boundary layers are satisfactory and the turbulence structure is not significantly modified. Spanwise divergence did not significantly affect either the Reynolds stress or turbulent triple-product distributions.

Nomenclature

$C_f/2$ = skin friction coefficient, $\tau_w/\frac{1}{2}\rho U_\infty^2$
H = boundary-layer shape factor, δ^*/Θ
P = pressure
R = radius of a hypothetical body of revolution
Re_Θ = momentum thickness Reynolds number
U, V, W = components of mean velocity
U_∞ = freestream velocity
u', v', w' = fluctuating components of velocity
u_τ = wall shear velocity, $\sqrt{\tau_w/\rho}$
u^+ = velocity in wall coordinates, U/u_τ
x, y, z = Cartesian coordinate system
y^+ = distance from wall in wall coordinates, yu_τ/ν
δ^* = boundary-layer displacement thickness, $\int_0^\infty (1 - U/U_\infty)\, dy$
δ_{99} = location where $U = 0.99U_\infty$, boundary-layer thickness
ν = fluid kinematic viscosity
ρ = fluid density
τ_w = wall shear stress
Θ = boundary-layer momentum thickness, $\int_0^\infty (U/U_\infty)(1 - U/U_\infty)\, dy$

Subscripts

edge = evaluated at outer edge of boundary layer ($y = \delta_{99}$)
wall = evaluated at the wall

Background

PREVIOUS studies have suggested that lateral divergence strongly affects boundary-layer development. The effects of divergence are often obscured, however, by other factors such as the streamwise pressure gradient and the streamwise curvature. For example, an adverse pressure gradient strongly influences the diverging boundary layer developing upstream of a flow blockage, and a strongly favorable pressure gradient affects the diverging boundary layer forming over a body of revolution with increasing radius. In contrast, the boundary layer that forms on a flat plate between common flow down vortex pairs experiences lateral divergence without the additional complications introduced by curvature and pressure gradients. Measurements made in this boundary layer can be used to clarify the effects of divergence on turbulent boundary-layer development.

A collaborative experimental study of zero-pressure-gradient diverging boundary layers was undertaken to isolate the effects of divergence from those of the streamwise pressure gradient and complex body geometry. Because it was also desirable to isolate the effects of divergence from those of the spanwise secondary velocities due to the vortices, the study was restricted to the boundary layer formed along the plane of symmetry between the two vortices of a pair with common flow down. The additional influence of a Reynolds number was removed by comparing boundary layers with similar momentum-thickness Reynolds numbers, one with and the other without spanwise divergence.

Smits et al.[1] studied the boundary layer on an axisymmetric cylinder-flared body that produced a combination of concave curvature and lateral divergence. Results indicated that spanwise divergence modified the boundary layer significantly, but it was not possible to fully separate the effects of divergence from those of concave curvature. Smits and Wood[2] discussed this difficulty further in their review article. In addition, they stated that in instances where concave curvature is present along with divergence, spanwise divergence can prevent the origination of roll cells that would otherwise accompany the concave curvature.

A number of researchers have studied diverging boundary layers formed upstream of symmetric obstacles mounted on a wall. The boundary layer experiences a strongly adverse pressure gradient and eventually separates. A recent study of three-dimensional boundary layers upstream of a wedge was performed by Anderson and Eaton.[3] They observed that the development of the boundary-layer mean and turbulence quantities along the centerline upstream of a wedge was similar to previous results obtained for several different types of ob-

Received Sept. 29, 1992; revision received May 26, 1993; accepted for publication May 30, 1993.

*Assistant Professor, Department of Aerospace Engineering. Member AIAA.
†Professor, Department of Mechanical Engineering. Member AIAA.
‡Assistant Research Professor. Member AIAA.

stacles. Based on their data and that of others, they concluded that the spanwise divergence did not strongly affect the turbulence structure of the boundary layer.

Patel and Baek[4] studied converging and diverging boundary layers on a body of revolution. On the upstream portion of the body, a diverging boundary layer formed in a strongly favorable pressure gradient. The measurements were limited because the boundary layer was very thin. They indicated the need for additional strain-rate data and turbulence measurements in a boundary layer with continuous flow divergence. Patel and Baek[5] presented calculations that included the effects of boundary-layer divergence. They determined that divergence led to an increase in the eddy viscosity and that including this effect in the turbulence model yielded more satisfactory results.

Saddoughi and Joubert[6] investigated the effects of prolonged streamline divergence on developing turbulent boundary layers. Using a uniquely shaped flow passage they investigated a boundary layer with two distinct regions: an upstream region with a combination of divergence and adverse pressure gradient and a downstream region with divergence but without a significant pressure gradient. They concluded that the boundary layer reaches a state of equilibrium in the presence of constant divergence. They attributed this to enhanced turbulent diffusion in the outer layer. Based on spectral measurements they concluded that divergence affects mainly the low-wave-number, large-scale motions in the boundary layer. Summarizing the previous literature, we find general agreement that divergence slows or reverses boundary-layer growth without modifying conventional mean flow similarity laws. However, there is no consensus on the effects of divergence on the turbulence structure because almost all of the experiments have mixed pressure gradient and divergence effects.

The continuity equation yields the following expression for spanwise divergence:

$$\frac{\partial W}{\partial z} = -\frac{\partial U}{\partial x} - \frac{\partial V}{\partial y} \tag{1}$$

In the two-dimensional boundary layers that we are studying, the streamwise gradients are small and the divergence is balanced largely by $\partial V/\partial y$. The momentum equation that describes the development of this layer is

$$U\frac{\partial U}{\partial x} + V\frac{\partial U}{\partial y} + \frac{\partial}{\partial x}\left(\frac{P}{\rho}\right) + \frac{\partial}{\partial y}\left(\overline{u'v'}\right) - \nu\frac{\partial^2 U}{\partial y^2} = 0 \tag{2}$$

where P is the pressure, ρ is the density, and ν is the kinematic viscosity. Because this study is limited to the plane of symmetry with no spanwise velocity, the spanwise momentum flux on the plane of symmetry is zero. The spanwise momentum equation, however, can be used to obtain an expression for the transport of the lateral divergence. Following Wheeler and Johnston[7] the transport of divergence is obtained by differentiating the z-momentum equation with respect to z and evaluating it at $z = 0$.

$$U\frac{\partial}{\partial x}\left(\frac{\partial W}{\partial z}\right) + V\frac{\partial}{\partial y}\left(\frac{\partial W}{\partial z}\right) + \left(\frac{\partial W}{\partial z}\right)^2 + \frac{\partial^2}{\partial z^2}\left(\frac{P}{\rho}\right) + \frac{\partial^2}{\partial y\,\partial z}\left(\overline{v'w'}\right) - \nu\frac{\partial^2}{\partial y^2}\left(\frac{\partial W}{\partial z}\right) = 0 \tag{3}$$

One approach to modeling the plane-of-symmetry boundary layer is to solve Eqs. (1-3) subject to appropriate boundary conditions imposed by the freestream. This requires a model for the shear stress components $\overline{u'v'}$ and $\overline{v'w'}$. The cross gradient of $\overline{v'w'}$ can probably be neglected, and the data presented below indicate that conventional models for $\overline{u'v'}$ will work well.

To determine the relative importance of divergence in the development of the boundary layer, the terms in the momentum integral equation for collateral, diverging flow can be evaluated (note that the present flow is not truly collateral but the difference is small near the centerline) as follows:

$$\underbrace{\frac{C_f}{2}}_{M_1} = \underbrace{\frac{\partial \Theta}{\partial x}}_{M_2} + \underbrace{\frac{\Theta}{U_\infty}(2+H)\frac{\partial U_\infty}{\partial x}}_{M_3} + \underbrace{\frac{\Theta}{U_\infty}\frac{\partial W_{\text{edge}}}{\partial z}}_{M_4} \tag{4}$$

We will restrict our study to those flows for which the contribution of the pressure gradient term M_3 may be neglected. Dividing this equation by $C_f/2$ gives us the following relationship between nondimensional variables:

$$\underbrace{\left(\frac{\Theta}{U_\infty}\frac{\partial W_{\text{edge}}}{\partial z}\middle/\frac{C_f}{2}\right)}_{S_1} + \underbrace{\left(\frac{\partial \Theta}{\partial x}\middle/\frac{C_f}{2}\right)}_{S_2} = 1 \tag{5}$$

where S_1 is the relative rate of growth of the boundary layer. The state of a diverging boundary layer may therefore be specified to a good approximation by either S_1 or S_2 and the momentum thickness Reynolds number (Re_Θ). The use of these nondimensional parameters allows us to compare our results to others in the literature in a sensible way.

Experimental Techniques

Two experimental facilities, one at Stanford University and one at Imperial College, were used to carry out the studies reported. In the Stanford experiment a diverging boundary layer was generated using a pair of half-delta-wing vortex generators mounted on the test wall at angle of attack (Fig. 1). The generators used in these studies were 2 cm high with a chord length of 5 cm. The spacing of the generators, measured between the midway point of the delta-wing chord, was varied from 2 to 14 cm. The angle of attack, which was measured between the vortex generators and the tunnel centerline, was varied between 6 and 24 deg. Secondary flow angles up to 20 deg were obtained using these half-delta-wing generators. The vortex generators were located 53 cm downstream of the boundary-layer trip at a point where the undisturbed boundary-layer thickness was 1.3 cm and the momentum-thickness Reynolds number was 1700. Boundary-layer growth resulted in a weak favorable pressure gradient with the freestream velocity increasing from 15.6 m/s at $X = 66$ cm to 16.4 m/s at the last measurement station ($X = 188$ cm). Pressure variation in the spanwise direction was very small ($C_p \ll 0.01$).

The experiment at Imperial College used a full delta wing mounted at an angle of attack to generate a vortex pair, which then interacted with the boundary layer developing on a flat test plate suspended in the test section farther downstream (Fig. 2). As a result of the interaction with the vortices, the boundary layer on the test plate between the vortices was strongly diverging. Two cases were studied. In case 1 the delta wing was mounted at a height such that the wake of the delta wing passed under the test plate whereas the vortices passed over the top. The boundary layer was strongly modified by the

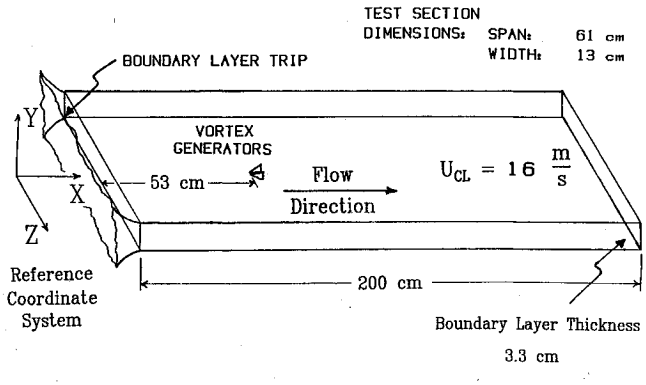

Fig. 1 Schematic of test facility with pair of half-delta-wing vortex generators used to study moderately diverging boundary layers.

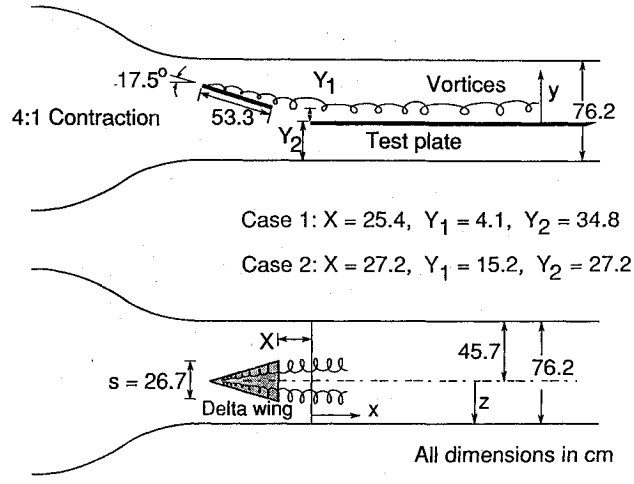

Fig. 2 Schematic of the full-delta-wing vortex generator and test plate used to study strongly diverging boundary layers.

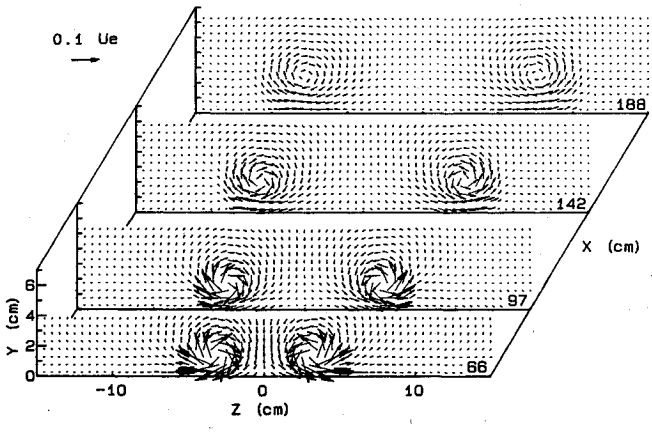

Fig. 3 Secondary flow vectors for a diverging boundary layer between an embedded vortex pair.

vortices and crossflow angles in the boundary layer exceeded 30 deg. In case 2 the delta wing was mounted much higher above the test plate so that the wake of the delta wing was more fully rolled up into the vortices before interaction with the boundary layer occurred. The boundary layer was less strongly modified by the vortices and crossflow angles were less than 15 deg.

Measurements were made using several different instrumentation systems. In the Stanford experiment, all three components of the mean velocity were measured using a miniature five-hole pressure probe that was calibrated using the scheme outlined by Westphal et al.[8] The mean velocity vector and the full Reynolds stress tensor were measured using an x-wire (crossed hot-wire anemometer). The wires were 5 μm, platinum-plated tungsten sensors with an active length of 1.25 mm. Details of this scheme are outlined by Pauley and Eaton[9] and a comprehensive uncertainty analysis can be found in Anderson and Eaton.[10] All ten triple products were calculated using a data reduction scheme presented by Cutler and Bradshaw.[11] The mean and fluctuating components of streamwise velocity were measured near the wall using a single-wire hot-wire probe with sensors similar to those used on the x-wire. The local skin friction magnitude and direction were measured using a surface fence gauge developed by Higuchi.[12]

In the Imperial College experiment, mean velocity profiles were obtained using a three-hole yaw probe and static pressure measurements from a surface tap. The yaw probe was aligned with the local mean velocity vector in yaw as described by Cutler and Bradshaw,[11,13] and the pitch angle was assumed to be small.

Results and Discussion

The secondary velocity field for the pair of vortices generated using a pair of half-delta-wing vortex generators spaced 4 cm apart at an 18-deg angle of attack is shown in Fig. 3. Details of the flowfield including the vorticity field, the streamwise decay of the vortex circulation, and the distortion of the vortices due to vortex/boundary-layer interaction were previously reported by Pauley and Eaton.[14] The vortices produce a small component of velocity directed toward the wall on the centerline. In addition, they produce an outward spanwise secondary flow directed away from the centerline that increases from zero on the centerline. Streamwise velocity contours shown in Fig. 4 show the distortion of the usual two-dimensional boundary layer resulting from the presence of the vortex pair. Comparing the boundary layer between the vortices with the undisturbed boundary layer outside of the vortex pairs shows the extent of thinning produced by the divergence.

A clear picture of the diverging flow is indicated by vectors of the secondary velocity in a plane parallel to the wall. These secondary flow vectors are shown in Fig. 5 near the outer edge of the thinned diverging boundary layer between the vortices. They indicate that the flow is diverging at angles up to 20 deg. The data in Figs. 3 and 5 were used to estimate the derivatives needed for the integral analysis described subsequently—cubic splines were computed through the data points and then differentiated analytically.

Profiles of mean velocity were measured with a single-wire hot wire resolving all of the log region and the buffer layer, extending down to the upper part of the viscous sublayer ($y^+ = 8$). Parameters such as the momentum-thickness Reynolds number and shape factor were calculated using the method of Coles,[15] and a log-law fit was made to determine the

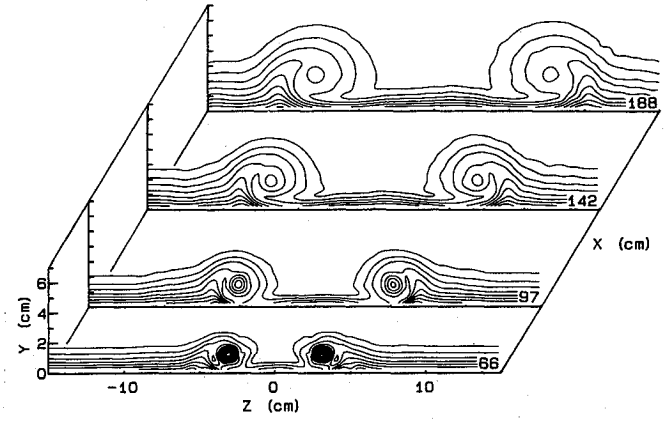

Fig. 4 Streamwise velocity contours for a diverging boundary layer between an embedded vortex pair; contour interval is 0.05 U_∞ with the outermost contour at δ_{99}.

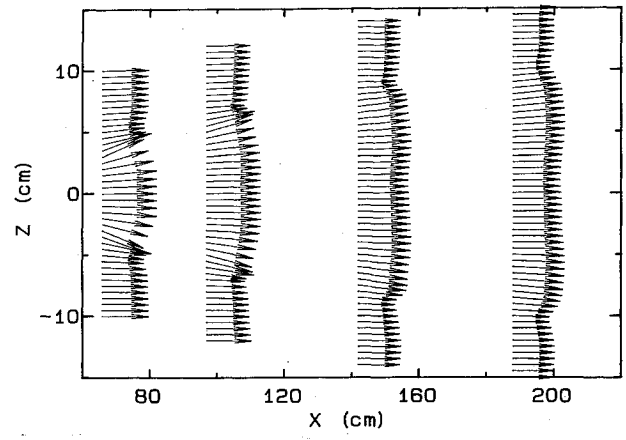

Fig. 5 Secondary flow vectors in a plane parallel to the wall near the edge of a diverging boundary layer at $Y = 0.75$ cm.

skin friction. The skin friction calculated using this fit was compared to the skin friction measured using the sublayer fence gauge and agreement within 2% was always observed. Scalar descriptors of the two-dimensional boundary layer and diverging boundary layer are tabulated in Table 1. To qualify the boundary layer, results for the two-dimensional, nondiverging case were compared with Coles[15] and with Eibeck and Eaton.[16] These results reported in Table 1 show excellent agreement between our boundary layer and that of others for similar Reynolds numbers.

The streamwise development of the momentum-thickness Reynolds number with divergence is shown in Fig. 6, and the development of the skin friction coefficient is shown in Fig. 7. Because the freestream velocity is nearly constant for all cases, comparison of the momentum-thickness Reynolds number development indicates a relative comparison of momentum-thickness growth between the diverging and nondiverging boundary layers. Initially the divergence strongly suppresses boundary-layer growth. Farther downstream the growth rate increases but is still well below the growth rate for an equivalent two-dimensional boundary layer of the same thickness.

To obtain different strengths of divergence on the centerline, the spacing of the vortices and the angle of attack of the generators were varied. Closer spacing of the generators produced more rapid divergence, a thinner boundary layer, and increased skin friction. Descriptors of the boundary layers are outlined in Table 1 for the vortex generator spacing study and for the vortex generator angle study. Boundary-layer profiles on the centerline between the vortices are plotted in wall coordinates in Fig. 8 for several generator spacings and in Fig. 9 for several angles of attack. These results indicate that the strong spanwise divergence observed upstream at $X = 97$ cm does not modify the usual logarithmic scaling observed in the logarithmic region of the boundary layer.

The relationship between the momentum-thickness Reynolds number and the local skin friction coefficient was compared to the normal behavior in two-dimensional, zero-pressure-gradient boundary layers. The results at the centerline for all of the half-delta-wing cases are shown in Fig. 10. All of the results (both on- and off-centerline) for the full-delta-wing case are presented in Fig. 11. The agreement between the data and the usual correlation for the variation of skin friction coefficient with Reynolds number ($C_f/2 = 0.0125 Re_\Theta^{-1/4}$) is generally good. This provides strong evidence backing up previous conclusions that divergence does not modify the normal similarity relations for the mean flow in the boundary layer based on local quantities such as the momentum thickness.

Each of the terms of the integral Eq. (4) have been computed at each of the streamwise locations along the centerline for the half-delta-wing case with 4-cm spacing and 18-deg angle of attack. The momentum integral balance between each of these terms, which is shown in Fig. 12, indicates that at the far-upstream location the divergence and skin friction terms are

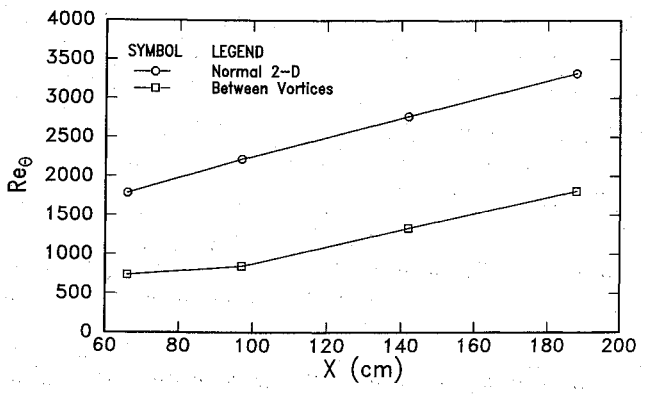

Fig. 6 Streamwise development of momentum-thickness Reynolds number with and without divergence.

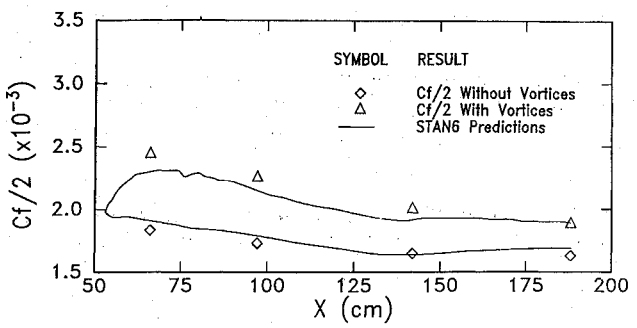

Fig. 7 Streamwise development of skin friction coefficient with and without divergence, also calculations from STAN6 using measured divergence.

Table 1 Two-dimensional and diverging boundary layer parameters and balance of terms in momentum integral equation (half-delta-wing cases)

X, cm	Space, cm	Angle, deg	U_∞, m/s	δ_{99}, cm	δ^*, cm	Θ, cm	H	Re_Θ	$\frac{C_f}{2}$ ×1000	$\frac{\partial\Theta}{\partial x}$ ×1000	$+\frac{\Theta}{U_\infty}(2+H)\frac{\partial U_\infty}{\partial x}$ ×1000	$+\frac{\Theta}{U_\infty}\frac{\partial W_{edge}}{\partial z}$ ×1000
66	—	—	15.62	1.59	0.249	0.176	1.415	1790	1.86			
97	—	—	15.86	1.88	0.307	0.215	1.427	2220	1.75			
142	—	—	15.74	2.29	0.377	0.268	1.408	2770	1.66			
188	—	—	16.37	2.67	0.423	0.308	1.373	3322	1.65			
Eibeck	—	—	—	2.67	0.424	0.310	1.37	3365	1.63			
Coles	—	—	—	—	—	—	1.38	3000	1.65			
66	4	18	15.62	0.737	0.104	0.073	1.431	739	2.52	0.06	0.14	2.77
97	4	18	15.81	0.746	0.121	0.081	1.488	822	2.36	0.66	0.03	1.46
142	4	18	15.68	1.19	0.188	0.131	1.440	1250	2.08	1.14	0.12	0.63
188	4	18	16.37	1.62	0.242	0.171	1.418	1808	1.89	0.74	0.63	0.43
97	4	6	15.75	0.877	0.127	0.087	1.459	897	2.34	—	—	2.84
97	4	12	15.86	0.734	0.113	0.076	1.495	780	2.41	—	—	2.18
97	4	18	15.81	0.746	0.121	0.081	1.488	822	2.36	0.66	0.03	1.46
97	4	24	15.83	0.838	0.128	0.087	1.466	897	2.31	—	—	1.21
97	2	18	15.77	0.99	0.102	0.070	1.458	720	2.59	—	—	2.35
97	3	18	15.75	0.61	0.103	0.068	1.516	703	2.43	—	—	1.82
97	4	18	15.81	0.746	0.121	0.081	1.488	822	2.36	0.66	0.03	1.46
97	6	18	15.72	1.13	0.170	0.118	1.435	1223	2.12	—	—	1.19
97	10	18	15.68	1.58	0.243	0.172	1.416	1772	1.89	—	—	0.65
97	14	18	15.76	1.69	0.275	0.194	1.415	1994	1.83	—	—	0.41

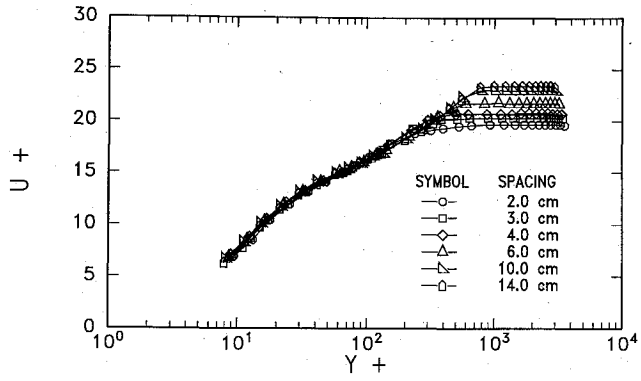

Fig. 8 Boundary-layer profiles in wall coordinates at $x = 97$ cm for several vortex generator spacings with fixed angle of attack.

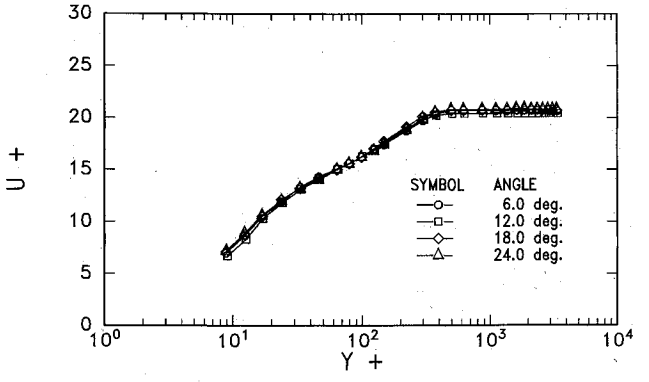

Fig. 9 Boundary-layer profiles in wall coordinates at $x = 97$ cm for several vortex generator angles of attack with fixed spacing.

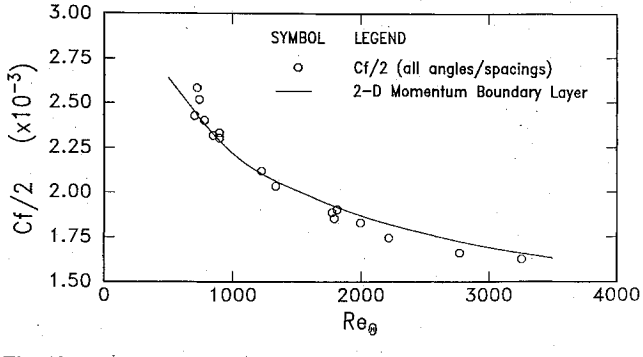

Fig. 10 Test of local similarity relationships for all cases using half-delta-wing vortex generators.

much larger than the other terms in the balance. As the vortices decay in strength, the level of divergence decreases and the growth of the momentum thickness becomes significant. At the most-downstream location the three terms on the right-hand side of the equation are nearly equal. There is a slightly favorable pressure gradient in the wind tunnel so that when the momentum thickness Θ becomes large enough (in the downstream region) the contribution of the pressure gradient term becomes significant. The divergence correction term is also reported for the spacing and angle study cases in Table 1.

Figures 13 and 14 show the four terms in the momentum integral equation on the centerline ($z = 0$) for both cases in the full-delta-wing experiment. In case 2 the first term in the momentum integral balance (which arises from the growth of the boundary layer) and the second term (which arises from the pressure gradient) are small compared to the other terms. Thus, the boundary layer at the centerline is the asymptotic boundary layer that develops in zero pressure gradient when the divergence is held constant. In case 1 the contributions of the growth term and the divergence term are comparable as a result of a steady reduction of the divergence moving downstream, but again the contribution of the pressure gradient term is, as expected, small. These full-delta-wing experiments have considered variation of the divergence parameter in the range $S_1 < 1$, and $400 < Re_\Theta < 3300$.

Bradshaw[17] determined that boundary layer turbulence is very sensitive to "extra rates of strain," that is, strain rates other than $\partial U/\partial y$. In the present case, the extra rate of strain is $\partial W/\partial z$. The ratio $(\partial W/\partial z)/(\partial U/\partial y)$ is reported in Table 2 for the centerplane boundary layer of all of the common flow-down pairs produced with the half-delta-wings. The strain rate ratios evaluated at $y = \delta_{99}/2$ indicate that these vortices

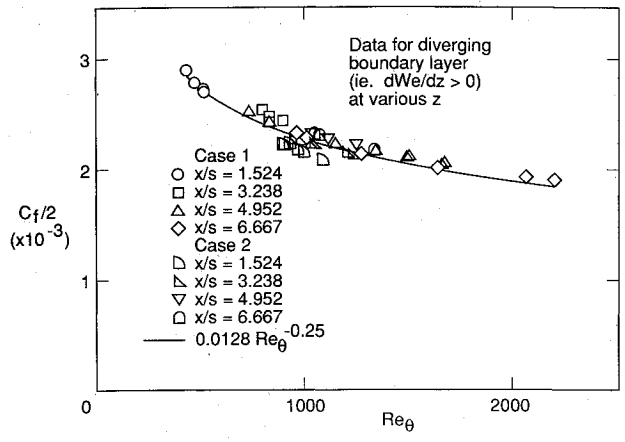

Fig. 11 Test of local similarity relationships for strong diverging boundary layers with delta-wing vortex generator.

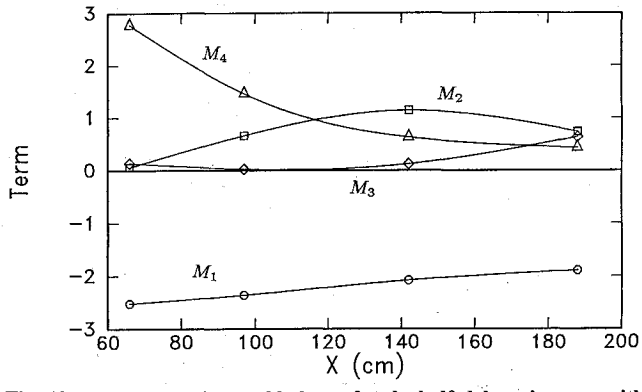

Fig. 12 Momentum integral balance for the half-delta-wing case with 18 deg angle of attack and 4-cm spacing.

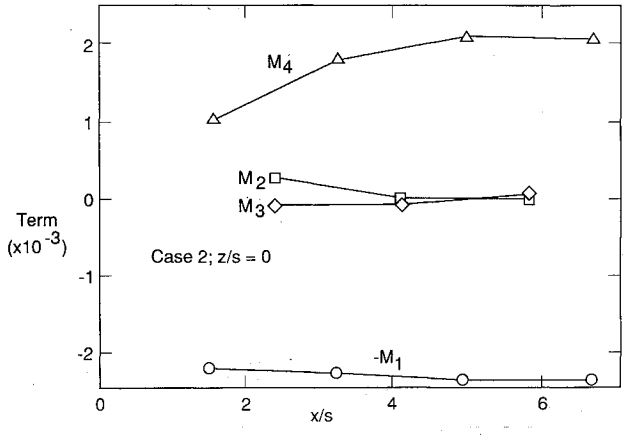

Fig. 13 Momentum integral balance for the full-delta-wing in the high position, case 2.

produce similar levels of the divergence ratio as observed by Smits et al.[1]

$$\left.\frac{\partial W}{\partial z}\middle/\frac{\partial U}{\partial y}\right|_{y=\delta_{99}/2} \approx 0.10$$

and Saddoughi and Joubert[6]

$$\left.\frac{\partial W}{\partial z}\middle/\frac{\partial U}{\partial y}\right|_{y=\delta_{99}/2} \approx 0.075$$

In addition, the ratio which uses the strain rate $\partial U/\partial y$ evaluated at the wall is reported. It might be argued that using the wall value is more universal as it avoids the arbitrary choice of the height at which to evaluate the derivatives, and this ratio enters directly into the momentum integral analysis. The typical ratio using the wall value is of the order 10^{-3}. Finally, the corresponding S_1 parameter defined in Eq. (5) is given in Table 2.

The diverging boundary layer at $x = 188$ cm had almost the same momentum-thickness Reynolds number as the normal two-dimensional boundary layer at $x = 66$ cm (all other flow conditions held constant). Figure 15 shows the streamwise velocity profiles for these two cases measured both with a single-wire hot wire and an x-wire. The boundary-layer profiles for these two cases are very similar, and good agreement is obtained between the two measurement systems. The turbulence intensity measured with the single wire for these two boundary layers is compared in Fig. 16. The turbulence intensity reaches its peak near the edge of the viscous sublayer and the two cases are in good agreement, well within the measurement uncertainty.

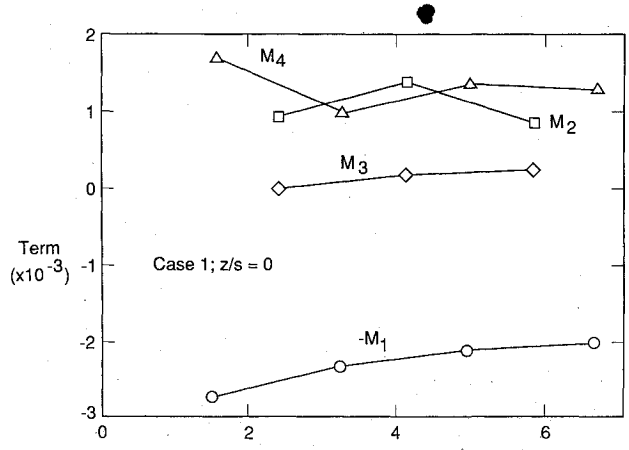

Fig. 14 Momentum integral balance for full-delta-wing in the low position, case 1.

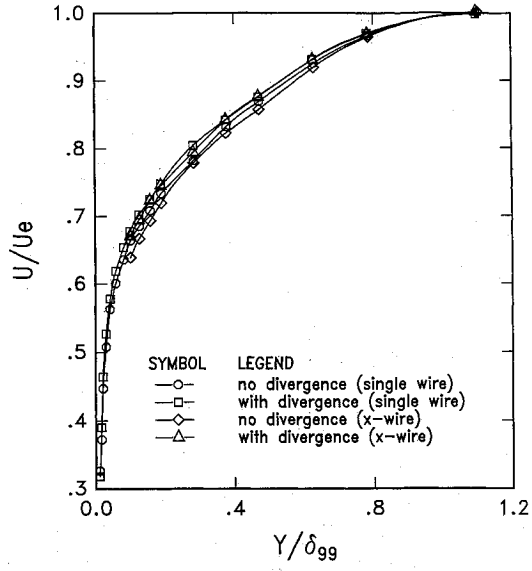

Fig. 15 Streamwise velocity profiles for a diverging boundary layer with $Re_\Theta = 1810$ ($X = 188$ cm) and a nondiverging boundary layer with $Re_\Theta = 1790$ ($X = 66$ cm).

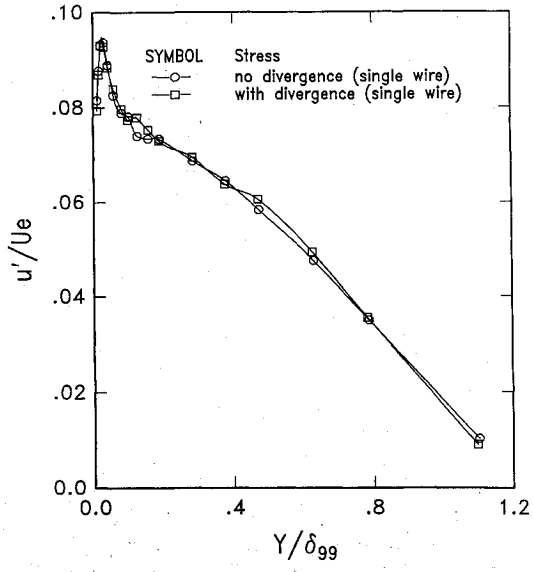

Fig. 16 Turbulence intensity profiles for a diverging boundary layer with $Re_\Theta = 1810$ and a nondiverging boundary layer with $Re_\Theta = 1790$ (half-delta-wing cases).

Table 2 Extra rate of strain parameters (half-delta-wing cases)

Case common flow down	At specification	$\frac{\partial W_{edge}}{\partial z}\left/\frac{\partial U}{\partial y}\right\|_{wall}$ $\times 10^{-3}$	$\left.\frac{\partial W}{\partial z}\middle/\frac{\partial U}{\partial y}\right\|_{y=\delta_{99}/2}$	$\left[\frac{\Theta}{U_\infty}\frac{\partial W_{edge}}{\partial z}\right]\Big/\frac{C_f}{2}$
4-cm spacing, 18 deg	$x = 66$ cm	1.48	0.086	1.10
4-cm spacing, 18 deg	$x = 97$ cm	0.74	0.046	0.62
4-cm spacing, 18 deg	$x = 142$ cm	0.23	0.016	0.30
4-cm spacing, 18 deg	$x = 188$ cm	0.13	0.011	0.23
4-cm spacing, $x = 97$ cm	6 deg	1.35	0.082	1.21
4-cm spacing, $x = 97$ cm	12 deg	1.16	0.061	0.90
4-cm spacing, $x = 97$ cm	18 deg	0.74	0.046	0.62
4-cm spacing, $x = 97$ cm	24 deg	0.59	0.038	0.52
$x = 97$ cm, 18 deg	2-cm spacing	1.26	0.146	0.91
$x = 97$ cm, 18 deg	3-cm spacing	1.07	0.047	0.75
$x = 97$ cm, 18 deg	4-cm spacing	0.74	0.046	0.62
$x = 97$ cm, 18 deg	6-cm spacing	0.46	0.035	0.56
$x = 97$ cm, 18 deg	10-cm spacing	0.19	0.018	0.34
$x = 97$ cm, 18 deg	14-cm spacing	0.11	0.009	0.22

Measurements of the full Reynolds stress tensor were made at each streamwise location with and without spanwise divergence. The profiles are shown for the two cases discussed earlier, to examine the influence of divergence on the development of the turbulence structure. The normal stresses and the primary shear stress are shown in Fig. 17. The Reynolds stresses are slightly higher for the diverging boundary layer. The difference between the two cases is no greater than a few percent, within the uncertainty of the measurements. Saddoughi and Joubert[6] also measured the Reynolds stresses with divergence. They compared their results with those of Erm[18] for a similar Reynolds number but without divergence. They observed that the Reynolds stresses at fixed y/δ_{99} increased gradually with streamwise distance under the influence of divergence and are higher than those observed for the two-dimensional boundary layer. They were not, however, able to conclusively determine whether to attribute this to lingering influence of an upstream pressure gradient or to divergence. If any effect is present due to divergence, their data suggest that normal stresses are increased rather than shear stresses. The streamwise normal component seems most affected (a maximum increase of 15% was observed). This trend was also observed in our data although the variation was weaker. The change observed in our data is not large enough to make a definitive conclusion about the direction of this change, given the uncertainty of a few percent in the measurements. Because our data sets, both with and without divergence, were obtained in the same facility with all tunnel run conditions held the same, it may be justifiable to attribute some significance to this weak trend that was observed in both laboratories. As their measurements have some uncertainty inherent in comparing results from two different laboratories, our observations can add further confidence in the trend that they observed, but suggest only a slight divergence-related modification.

A slight increase in magnitude due to divergence was observed for the triple products which are shown in Fig. 18. The trends and magnitudes of the quantities with and without divergence are similar and strong statements based on the level of the differences observed would stand on questionable footing due to the moderate uncertainty in these triple correlations. In the outer-half of the boundary layer where the levels of uncertainty in the measurements are the lowest, the triple products $\overline{u'^3}$, $\overline{u'^2v'}$, and $\overline{u'v'^2}$ are consistently larger in the diverging boundary layer. This trend is also in agreement with Saddoughi and Joubert but again the magnitude of the difference is small. The other triple products are quite small. In general, no dramatic modification of the boundary-layer structure due to divergence is observed. This contradicts observations of several previous experiments where it was not possible to fully isolate divergence effects.

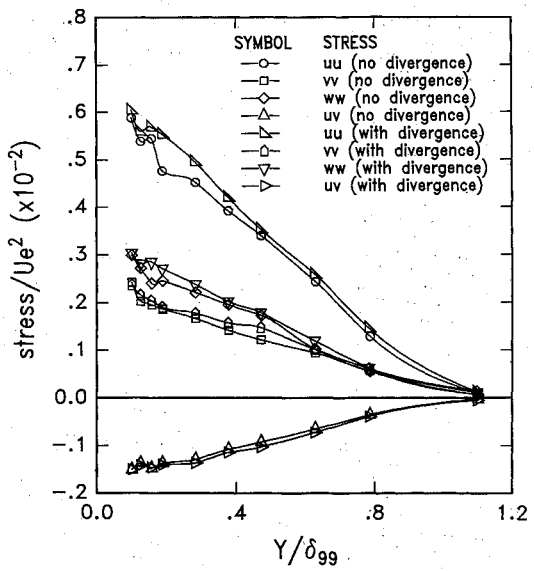

Fig. 17 Reynolds normal stresses and shear stress for a diverging boundary layer with $Re_\Theta = 1810$ and a nondiverging boundary layer with $Re_\Theta = 1790$ (half-delta-wing cases).

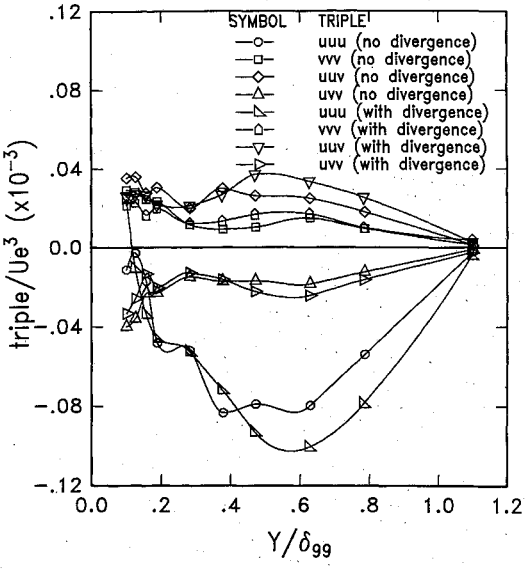

Fig. 18 Turbulent triple products $\overline{u'^3}$, $\overline{v'^3}$, $\overline{u'^2v'}$, and $\overline{u'v'^2}$ for a diverging boundary layer with $Re_\Theta = 1810$ and a nondiverging boundary layer with $Re_\Theta = 1790$.

The results of Smits et al.[1] have indicated that the effect of the extra rate-of-strain $\partial W/\partial z$ on turbulence model "constants" such as nondimensional eddy viscosity is large (an increase of a factor of two or more). It was suggested that the effects can be correlated by the extra rate-of-strain parameter

$$\left.\frac{\partial W}{\partial z}\middle/\frac{\partial U}{\partial y}\right|_{y=\delta_{99}/2}$$

In the Smits et al. layer this extra rate-of-strain parameter is 0.10 ($S_1 \approx 1.5$, $Re_\Theta \approx 4000$), which is similar in magnitude to the divergence seen at the upstream locations in this experiment ($S_1 \approx 1.1$). The results of Smits et al. are not conclusive due to the additional effects of concave curvature at the upstream locations. Note that for the mean flow results S_1 varies in the range of 0–1.2 and so the conclusions concerning these are valid for stronger lateral divergence.

STAN6, a finite-difference boundary layer code written by W. M. Kays at Stanford University, was used to determine if the mean divergence effects could be captured by a two-dimensional calculation with a divergence correction. The momentum integral equation for a boundary layer forming over a body of revolution as reported by Kays and Crawford[19] is

$$\frac{C_f}{2} = \frac{\partial \Theta}{\partial x} + \frac{\Theta}{U_\infty}(2+H)\frac{\partial U_\infty}{\partial x} + \underbrace{\frac{\Theta}{R}\frac{\mathrm{d}R}{\mathrm{d}x}}_{M_4^*} \tag{6}$$

This equation is similar to Eq. (4) with the exception of the term M_4^*, which can be related to term M_4 in the previous equation. This results in the following relationship between the divergence of a flat-plate boundary layer and the radius of a hypothetical body of revolution over which a diverging boundary layer forms:

$$\frac{\mathrm{d}R}{\mathrm{d}x} = \left(\frac{R}{U_\infty}\right)\frac{\mathrm{d}W_{\mathrm{edge}}}{\mathrm{d}z} \tag{7}$$

Using the divergence measurements for the centerline of the half-delta-wing case shown in Figs. 3 and 4, a calculation of the skin friction development was performed for a hypo-

thetical body of revolution. The results are shown in Fig. 7. By modeling the divergence as an equivalent change in radius, this two-dimensional boundary-layer code based on a mixing length turbulence model was quite satisfactory. This further supports the conclusion that the divergence, while strongly modifying the mean boundary-layer development, does not significantly modify the turbulence structure of the boundary layer.

Conclusions

The effects of divergence on the formation of a turbulent boundary layer has been studied. Measurements indicate that the divergence controls the rate of development of the boundary layer and that large divergence significantly retards boundary-layer growth and enhances skin friction. Even in the presence of boundary-layer divergence the local similarity relationships for two-dimensional boundary layers without divergence are satisfactory. The boundary-layer profiles collapse on the log-law relationship. The balance of terms in the usual momentum integral equation must be supplemented by an additional term to account for the effects of divergence. These conclusions are in general agreement with previous work cited above.

Disagreement exists in the literature regarding the effects of this divergence on the turbulence structure. This is possibly due to the additional complications introduced by streamwise curvature and streamwise pressure gradient found in the different experimental facilities used to generate diverging boundary layers. In the present experiments with a zero streamwise pressure gradient and $S_1 = 1.1$, it was found that spanwise divergence did not significantly affect the Reynolds stress tensor and the turbulent triple products. It is possible that in strongly diverging boundary layers (i.e., greater S_1) there may be a significant effect of divergence on turbulence structure. To date, however, there is no conclusive evidence of this effect.

Acknowledgments

We gratefully acknowledge the financial support of the Department of Energy Basic Energy Sciences Program, Contract DEFG0386ER-13608, who supported the work at Stanford, and the support of the NASA Ames Research Center, Contract NAGw-581, who supported the work at Imperial College. The work conducted at Imperial College was supervised by Peter Bradshaw, and we are grateful for his considerable contributions to this paper.

References

[1]Smits, A. J., Eaton, J. A., and Bradshaw, P., "The Response of a Turbulent Boundary Layer to Lateral Divergence," *Journal of Fluid Mechanics,* Vol. 94, Pt. 2, 1979, pp. 243–268.

[2]Smits, A. J., and Wood, D. H., "The Response of Turbulent Boundary Layers to Sudden Perturbations," *Annual Review of Fluid Mechanics,* Vol. 17, 1985, pp. 321–358.

[3]Anderson, S. D., and Eaton, J. K., "Reynolds Stress Development in Pressure-Driven Three-Dimensional Turbulent Boundary Layers," *Journal of Fluid Mechanics,* Vol. 202, 1989, pp. 263–294.

[4]Patel, V. C., and Baek, J. H., "Boundary Layers in Planes of Symmetry, Part I: Experiments in Turbulent Flow," *AIAA Journal,* Vol. 25, No. 4, 1987, pp. 550–559.

[5]Patel, V. C., and Baek, J. H., "Boundary Layers in Planes of Symmetry, Part II: Calculations for Laminar and Turbulent Flows," *AIAA Journal,* Vol. 25, No. 6, 1987, pp. 812–818.

[6]Saddoughi, S. G., and Joubert, P. N., "Lateral Straining of Turbulent Boundary Layers. Part 1. Streamline Divergence," *Journal of Fluid Mechanics,* Vol. 229, 1991, pp. 173–204.

[7]Wheeler, A. J., and Johnston, J. P., "An Assessment of Three-Dimensional Turbulent Boundary Layer Prediction Methods," *Journal of Fluids Engineering,* Vol. 95, 1973, pp. 415–421.

[8]Westphal, R. V., Pauley, W. R., and Eaton, J. K., "Interaction Between a Vortex and a Turbulent Boundary Layer, Part I: Mean Flow and Turbulence Properties," NASA TM-88361, Jan. 1987.

[9]Pauley, W. R., and Eaton, J. K., "The Fluid Dynamics and Heat Transfer Effects of Streamwise Vortices Embedded in a Turbulent Boundary Layer," Stanford Univ., Thermosciences Div. Rept. MD-51, Stanford, CA, Aug. 1988.

[10]Anderson, S. D., and Eaton, J. K. "An Experimental Investigation of Pressure Driven Three-Dimensional Turbulent Boundary Layers," Stanford Univ., Thermosciences Div. Rept. MD-49, Stanford, CA, June 1987.

[11]Cutler, A. D., and Bradshaw, P., "A Crossed Hot-Wire Technique for Complex Turbulent Flows," *Experiments in Fluids,* Vol. 12, 1991, pp. 17–22.

[12]Higuchi, H., "A Miniature Directional Surface-Fence Gage for Three-Dimensional Turbulent Boundary Layer Measurements," AIAA Paper 83-1722, June 1983.

[13]Cutler, A. D., and Bradshaw, P., "Vortex/Boundary-Layer Interactions," AIAA Paper 89-0083, Jan. 1989.

[14]Pauley, W. R., and Eaton, J. K., "Experimental Study of the Development of Longitudinal Vortex Pairs Embedded in a Turbulent Boundary Layer," *AIAA Journal,* Vol. 26, No. 7, 1988, pp. 816–823.

[15]Coles, D. E., "The Young Person's Guide to the Data," *Proceedings: Computation of Turbulent Boundary Layers, AFOSR, IFP/Stanford Conference,* Vol. II, Stanford Univ., Stanford, CA, Aug. 1968, pp. 1–45.

[16]Eibeck, P. A., and Eaton, J. K., "The Effects of Longitudinal Vortices Embedded in a Turbulent Boundary Layer on Momentum and Thermal Transport," *Proceedings of the Eighth International Heat Transfer Conference* (San Francisco, CA), Vol. 3, Washington, DC, 1986, pp. 1115–1120.

[17]Bradshaw, P., "Review-Complex Turbulent Flows," *Journal of Fluids Engineering,* Vol. 97, 1975, p. 146.

[18]Erm, L. P., "Low Reynolds Number Turbulent Boundary Layers," Ph.D. Thesis, Dept. of Mechanical Engineering, Univ. of Melbourne, Melbourne, Australia, 1988.

[19]Kays, W. M., and Crawford, M. E., *Convective Heat and Mass Transfer,* McGraw-Hill, New York, 1980.